

Chain-Length Dependent Stationary and Time-Resolved Spectra of α -OligothiophenesAiping Yang[†]

Department of Physics, University of Tokyo, 7-3-1 Hongo, Bunkyo, Tokyo 113, Japan

Masami Kuroda and Yotaro Shiraishi

Fuji Electric Corporate Research and Development, Ltd., Yokosuka, Kanagawa 240-01, Japan

Takayoshi Kobayashi*

Department of Physics, University of Tokyo, 7-3-1 Hongo, Bunkyo, Tokyo 113, Japan

Received: November 4, 1997; In Final Form: March 3, 1998

By analyzing stationary absorption and fluorescence spectra of several α -oligothiophenes in dichloromethane at room temperature, the $S_1 \leftarrow S_0$ zero-zero transition energies and Huang–Rhys parameters are determined. Reorientational behaviors of the α -oligothiophenes in dichloromethane are also investigated by femtosecond time-resolved fluorescence spectroscopy. The reorientational relaxation observed for each α -oligothiophene in its first excited state is interpreted in terms of revolution of a hydrodynamic prolate ellipsoid of which the emission transition dipole is aligned along the long molecular axis. Our results show that a hydrodynamic slip model could successfully explain the reorientation times of α -terthiophene, α -quaterthiophene, and α -quinquethiophene in dichloromethane at 288 K, by modeling these molecules as prolate ellipsoids with dimensions consistent with their van der Waals volumes.

1. Introduction

Polythiophenes and thiophene oligomers have been extensively studied both experimentally and theoretically because of their possible applications in electronic and optoelectronic devices.^{1–28} Studies of stationary and time-resolved spectra of α -oligothiophenes in solution can lead to a better understanding of their intrinsic electronic and conformational properties. Further, the study of chain-length dependence of these properties could provide useful insight into the nature of photoexcitations in more complex polythiophenes.

Unlike their fluorescence spectra, the lowest-energy absorption bands of α -oligothiophenes (T_n for $n = 3–6$, n denotes the number of the thiophene rings) dissolved in common solvents at room temperature, are generally broad and do not show any observable vibrational structure. However, at low temperature, the absorption spectra reveal well-resolved vibrational progressions, and noticeable shifts of the absorption maxima on cooling have been observed.^{29–32} These phenomena are thought to relate with molecular backbone conformations. The attention of many workers has been focused on the conformational structures of α -oligothiophenes, involving the internal rotational potential of the compounds as well as the effect of inter-rings torsional angles on the electronic structures.^{33–39} Such studies addressed the questions whether α -oligothiophene in gas or solution phase is present as a single *anti*-like conformer,^{34,36} or as a mixture of both *anti*- and *syn*-like conformers,^{37,38} or as an ensemble of various rotamers.

Recently, Belletete et al.³⁹ have performed semiempirical calculations on α -bithiophene and α -terthiophene to determine their electronic transition energies as a function of inter-rings

torsional angles. They proposed a joint theoretical and experimental method to elucidate the conformations of α -oligothiophenes in their respective ground and first excited singlet and triplet states.⁴⁰ Therefore, the knowledge of the $S_1 \leftarrow S_0$ 0–0 transition energies and the vibrational structures, which cannot be read directly from the absorption spectra, may provide useful information and physical insight into the intrinsic electrical properties and the geometric conformations of α -oligothiophenes in solutions.

The time-resolved spectra of α -oligothiophenes in solutions have been studied by several authors.^{41–45} For example, Chosrovian et al.⁴¹ studied the size-dependent transient behaviors of thiophene oligomers by picosecond absorption spectroscopy. Charra et al.⁴² studied the picosecond photoinduced dichroism of α -oligothiophenes in solutions by using a Kerr ellipsometry configuration. Grebner and co-workers⁴³ applied femtosecond optical pump-and-probe spectroscopy to didecyl-sexithiophene in solution using one- and two-photon excitations. Lanzani et al.⁴⁴ performed pump–probe measurements on a substituted α -conjugated sexithiophene in solution to study the femtosecond and picosecond time evolution of the excited-state dynamics. Kanemitsu et al.⁴⁵ measured the fluorescence decay times of α -oligothiophenes in solution with a 30-ps resolution. Moreover, several authors measured fluorescence and the intersystem-crossing quantum yields of α -oligothiophenes in various solvents.^{32,46,47} Previously we investigated reorientational behavior of α -terthiophene in dichloromethane (CH_2Cl_2) at room temperature.⁴⁸

In the present study, we determine the $S_1 \leftarrow S_0$ 0–0 transition energies of T_n for $n = 3, 4, 5$, and 6 in dichloromethane at room temperature from negative second derivatives of the broad absorption spectra. Based on this result, a value of the $S_1 \leftarrow S_0$ 0–0 transition energy of polythiophene is estimated to be

* Corresponding author. E-mail: takakoba@phys.s.u-tokyo.ac.jp.

[†]E-mail: yang@femto.phys.s.u-tokyo.ac.jp.

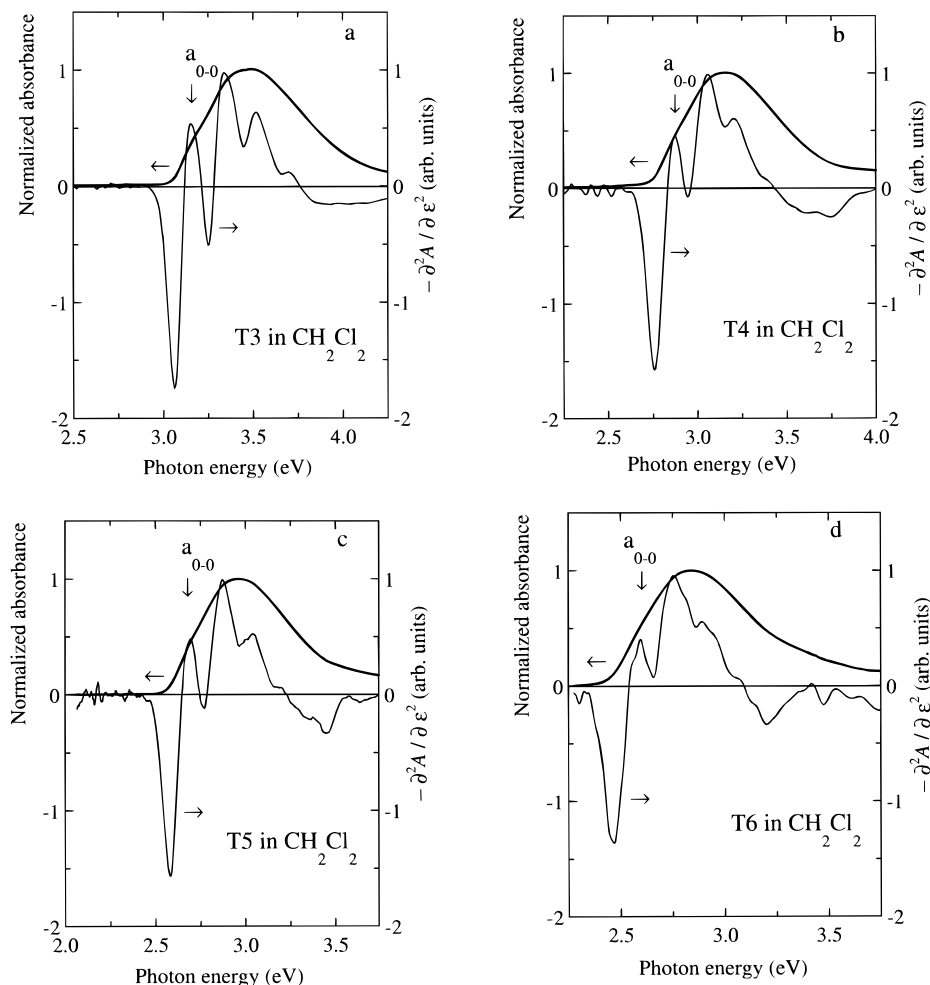


Figure 1. Normalized absorption spectra (thick solid lines) and their negative second derivatives (thin solid lines) of α -oligothiophenes in dichloromethane solution at room temperature: (a) α -terthiophene (T3), (b) α -quaterthiophene (T4), (c) α -quinquethiophene (T5), and (d) α -sexithiophene (T6).

~ 2.02 eV. We also perform the Huang–Rhys analysis^{49,50} of the fluorescence spectra of T_n ($n = 3–6$), showing that the Huang–Rhys parameter decreases with the chain length. Further, we study reorientational dynamics of the compounds and demonstrate that a hydrodynamic model with a slip-boundary condition could successfully explain the reorientation times of T_n for $n = 3–5$ in dichloromethane at room temperature.

2. Experimental Section

The absorption spectra were recorded with a spectrometer (Shimadzu, UV-3101PC). The stationary fluorescence and fluorescence excitation spectra were measured with a fluorescence spectrometer (Hitachi, F-4500), and corrections were made for spectral sensitivity of the entire measuring system.

For femtosecond time-resolved measurements, a mode-locked Ti:sapphire laser (NJA-4, Clark-MAX) pumped by a CW argon ion laser (INNOVA 300, Coherent) was employed to produce optical pulses with a wavelength centered at 800 nm and a repetition rate of 100 MHz. The average output power from the Ti:sapphire laser is ~ 600 mW. The fundamental beam was frequency doubled in a 1-mm thick β -barium borate (BBO) crystal to obtain a 400-nm excitation pulse of ~ 230 fs duration. The excitation pulse separated from the fundamental gate pulse by a dichroic beam-splitter was focused into a 1-mm path length glass cell containing the α -oligothiophene solution, and the

average excitation power was ~ 3 mW (3×10^{-11} J/pulse). The fluorescence from the sample was collected using a microscope objective lens ($\times 10$) and focused into a 0.5-mm thick BBO crystal to be mixed with the fundamental pulse for the type I phase-matching sum-frequency generation. The up-converted signal passed through a 0.25-m monochromator (Ritsu, MC-25) and was detected with a photomultiplier (Hamamatsu, R-2693P) and a single-photon counter (Hamamatsu, M3949).⁵¹ The time resolution of the system was estimated to be ~ 250 fs from the full width at half-maximum of the cross-correlation trace between the excitation and the fundamental pulses.

Concentrations of T3, T4, and T5 CH_2Cl_2 solutions used for the stationary and time-resolved measurements were $\sim 1 \times 10^{-4}$ mol/dm³. The solubility of the T6 molecule in common solvents is very low. The concentration of T6 CH_2Cl_2 solution used $\sim 10^{-5}$ mol/dm³. No dependence of fluorescence lifetimes and spectra on concentration in the range 10^{-3} – 10^{-5} mol/dm³ was registered.⁴¹ To avoid inner-filter effects and reabsorption processes, the 1-mm path length cell was used for the measurements of the fluorescence spectra.

3. Results and Discussion

Absorption and Second-Derivative Spectra. The normalized absorption spectra of T_n for $n = 3–6$ in dichloromethane are respectively shown in Figures 1(a)–(d). The absorption spectra are broad and structureless. To gain more information

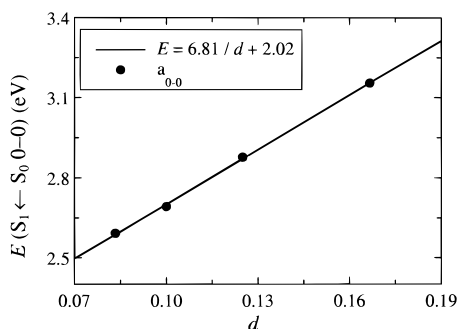


Figure 2. $S_1 \leftarrow S_0$ 0–0 transition energies (filled circles) of α -oligothiophenes as a function of $1/d$ (where d is the number of double bonds). The solid line is the experimental fit using eq 1 in the text.

on the vibrational structures, we calculate the negative second derivatives (NSD) of the absorption spectra (lowest-energy bands). As shown in Figures 1(a)–(d), two peaks and two small shoulders are present in the NSD spectra of all the samples. For T3, the peaks in the NSD spectrum are located at 3.15, 3.34, 3.52, and 3.70 eV. The energy difference between the adjacent peaks is in the order of 0.18–0.19 eV, indicating the strong coupling between the electronic π – π^* transition and a C=C stretching vibrational mode. The lowest-energy peaks in the NSD, labeled as a_{0-0} in Figures 1(a)–(d), are assigned to the $S_1 \leftarrow S_0$ 0–0 transitions of T3, T4, T5, and T6, respectively.⁴⁸

Chain-Length Dependence of the $S_1 \leftarrow S_0$ Zero–Zero Transition Energy. As can be recognized from Figures 1(a)–(d), the absorption spectrum is progressively red shifted with increasing the chain length. As the chain length grows, the delocalization of π electrons is increased, resulting in the reduction of the π – π^* transition energy. To show this effect, the $S_1 \leftarrow S_0$ 0–0 transition energies are plotted as a function of $1/d$ in Figure 2 (d is the number of double bonds).⁵² The 0–0 transition energies (in eV) of T3–T6 in dichloromethane at room temperature are well fitted by

$$E_{0-0}^a = 6.81/d + 2.02 \quad (1)$$

Extrapolation of eq 1 to polythiophene with an infinite conjugation length gives a value of the 0–0 transition energy of 2.02 eV. Since unsubstituted polythiophene cannot be dissolved in common solvents, the experimental value of the 0–0 transition energy of the polythiophene in solution is absent in the literature. Chung and co-workers⁵³ studied the absorption spectrum of a polythiophene film prepared electrochemically and determined the 0–0 transition energy to be 2.1 eV. The small difference between their value and ours may be due to differences in refractive indexes, effective conjugation lengths, and conformational structures of the polythiophene samples studied.

Fluorescence Spectra. The fluorescence spectra of T_n for $n = 3, 4, 5$, and 6 in dichloromethane at room temperature are shown in Figure 3(a). The fluorescence spectrum of each T_n shows pronounced vibrational structures. Two distinct peaks, which respectively correspond to the $S_1 \rightarrow S_0$ 0–0 and $S_1 \rightarrow S_0$ 0–1 transitions, are observed. The presence of the vibrational structures in the fluorescence spectrum, unlike its absorption spectrum, indicates that the absorption and emission processes at T_n are associated with the different molecular conformations. In the ground state, the molecular skeleton of T_n is nonplanar, whereas in the excited state, the molecular geometry is characterized by a more rigid planar conformation.^{32,48} This difference in the molecular skeleton is associated

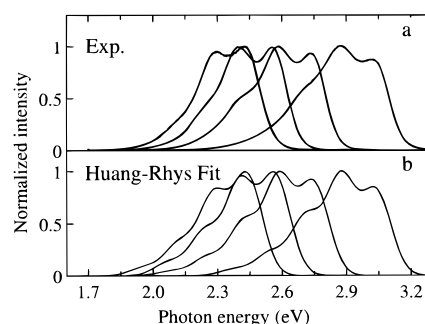


Figure 3. (a) Normalized experimental fluorescence spectra and (b) Huang–Rhys fits of the fluorescence spectra of α -oligothiophenes T_n for $n = 3, 4, 5$, and 6 in dichloromethane solution at room temperature.

TABLE 1: Huang–Rhys Parameters (S), Phonon Energies ($h\nu$), Damping Factors (Γ), and Relaxation Energies (E_{rel}) Obtained from Huang–Rhys Analysis of Experimental Fluorescence Spectra of α -Oligothiophenes T_n ($n = 3, 4, 5$, and 6) in Dichloromethane

parameter	T3	T4	T5	T6
S	1.060	1.010	0.916	0.804
$h\nu$ (eV)	0.165	0.165	0.165	0.165
Γ (eV)	0.081	0.077	0.078	0.080
E_{rel} (eV)	0.175	0.167	0.151	0.133

with a transition of the electronic structure from an aromatic form in the ground state to a quinoidal form in the excited state.^{32,48}

Huang–Rhys Parameters. We perform the Huang–Rhys analysis of the fluorescence spectrum of T_n within Franck–Condon approximations. The fluorescence spectrum consists of several vibrational sidebands displaced by a phonon energy $h\nu_j$, and the distribution of peak heights in the fluorescence spectrum follows the Poisson distribution,

$$I(n_j) = S_j^{n_j} e^{-S_j} / n_j! \quad (2)$$

Here S_j is a dimensionless Huang–Rhys parameter of the j th vibrational mode, which measures a displacement of the equilibrium position of the excited state relative to the ground state.⁴⁹ The fluorescence spectra of all T_n studied are analyzed by assuming a single active vibrational mode coupled with the electronic transition as well as a Gaussian line shape with a damping factor Γ (line width broadening parameter). The simulated spectra, which match well the experimental results, are plotted in Figure 3(b), and the optimized parameters are listed in Table 1. Our results show that the value of S monotonically decreases as the chain grows, which is consistent with the fact that the relative height of the zero-vibrational peak in the fluorescence spectrum increases with n [see Figure 3(a)]. This result reflects the increasing delocalization of electronic wave functions with increasing the chain length.⁵⁰ We also calculate geometrical relaxation energies of T_n using the relation $E_{\text{rel}} = S h\nu$. The relaxation energy of each T_n studied, as listed in Table 1, is in the region 0.13–0.18 eV, which is in good agreement with that predicted by Beljonne et al.¹⁵

Time-Resolved Fluorescence. Figure 4 shows time-resolved fluorescence profiles of T3, T4, and T5 in dichloromethane at 288 K. When the excitation light is parallel-polarized with respect to the detected fluorescence, the fluorescence decay of each T_n is nonexponential and can be well fitted by a biexponential function,

$$I_{\parallel}(t) = c_1 \exp(-t/\tau_1) + c_2 \exp(-t/\tau_2) \quad (3)$$

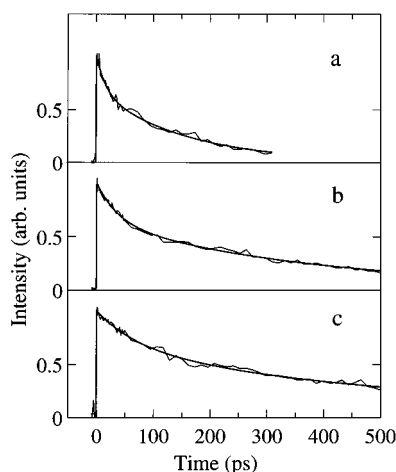


Figure 4. Time-dependent fluorescence intensities of α-oligothiophenes in dichloromethane solution at 288 K when the polarization of excitation light is parallel to the polarization of the measured fluorescence: (a) α-terthiophene (T3), (b) α-quaterthiophene (T4), and (c) α-quintothiophene (T5). The thick solid lines are biexponential fits to the experimental data (thin solid lines).

TABLE 2: Axial Ratios (ρ), van der Waals Volumes (V), Hydrodynamic Parameters (g , f), Fluorescence Decay Times (τ_n , τ_2), and Reorientation Times (τ^{or}) of α-Oligothiophenes T_n ($n = 3-5$) in Dichloromethane ($\eta = 0.499$ cP^a) at 288 K and χ^2 Values of the Fits

parameter	T3	T4	T5
ρ	2.58	3.44	4.30
V (Å ³)	193.3	254.2	315.1
g	0.511	0.360	0.267
f	0.375	0.520	0.610
$\tau_n = \tau_1$ (ps)	160 ± 10	390 ± 40	610 ± 80
τ_n^b (ps)	150 ± 10	530 ± 50	870 ± 90
τ_n^c (ps)	160	370	650
τ_2 (ps)	16 ± 3	36 ± 8	70 ± 10
τ_{exp}^{or} (ps)	18 ± 4	40 ± 10	80 ± 20
τ_{slip}^{or} (ps)	17.8	46.1	90.4
τ_{stick}^{or} (ps)	47.5	88.7	148.2
χ^2	1.04	1.02	1.01

^a From ref 60. ^b See ref 46. ^c Estimated from Figure 5 in ref 45.

where $I_{||}(t)$ is the intensity at time t , and the subscript $||$ denotes the polarization of the emission component parallel to the polarization of the excitation light. The time constants of the slow (τ_1) and the fast (τ_2) decay components obtained from fitting are listed in Table 2. The χ^2 values that judge quality of the fits are close to unity, as listed in Table 2. We have investigated the time-resolved fluorescence of T4 in dichloromethane under a magic-angle polarization condition as well as in a more viscous solvent of the ethyleneglycol and dimethyl sulfoxide mixture (1/1 volume ratio) when the excitation light was parallel-polarized with respect to the detected fluorescence. In both cases, we observed an exponential decay with a single time constant very close to that of the slow decay component of T4, as depicted in Figure 4.

Based on the results of the present and previous work,⁴⁸ we suggest that the fast decay component of each T_n studied is associated with the molecular rotational diffusion in dichloromethane. The slower decay component is assigned to the radiative relaxation $S_1 \rightarrow S_0$, which is almost independent of the solvent viscosity. The values of the slow decay time constants reported here are comparable to those reported in refs 45 and 46 (see Table 2). Like the earlier experimental results,^{45,46} the $S_1 \rightarrow S_0$ radiative decay time $\tau_n (= \tau_1)$ is increased with the chain length. The radiative and nonradiative

decay processes of α-oligothiophenes in solutions have already been investigated by several authors.^{32,46,47} Recently, Oelkrug et al.⁴⁷ measured the fluorescence and intersystem crossing quantum yields of several α-oligothiophenes in dichloromethane. They suggested that the dominant nonradiative decay route at T_n in solution competing with fluorescence is the process of triplet formation.

The time-dependent fluorescence intensities at various emission photon energies have been measured for T3, T4, and T5. No dependence of the fluorescence decay feature on the detected emission photon energy was observed within our experimental uncertainty. It is also found that no dependence of the fluorescence spectra on the excitation photon energy or of the excitation spectra on the detected emission photon energy for T3, T4, T5 as well as T6 in dichloromethane was observed at room temperature. The aforementioned results may lead to the conclusion that the observed fluorescence spectrum of each T_n in solution is attributed to a single conformer. However, recent theoretical results showed that both the $S_1 \leftarrow S_0$ transition energies and oscillator strengths of the syn and anti conformers are nearly identical for T2 and T3 molecules.⁴⁰ For example, the difference in the $S_1 \leftarrow S_0$ 0-0 transition energies of syn- and anti-planar conformers for T3 molecule is <0.01 eV.⁴⁰ Thus, on the basis of the aforementioned measurements alone, we are not able to draw the conclusion about the number of the conformers that contribute to the observed spectra due to the limitation of our experimental resolution.

Reorientation Time and Fluorescence Initial Anisotropy.

The fluorescence anisotropy for linear polarized excitation light is defined by

$$r(t) = \frac{I_{||}(t) - I_{\perp}(t)}{I_{||}(t) + 2I_{\perp}(t)} \quad (4)$$

where the subscripts denote the polarization of the emission component, which is parallel ($||$) or perpendicular (\perp) to the polarization of the excitation light. According to a hydrodynamic model,^{54,55} the fluorescence anisotropy decay, from a molecule that has a single geometrical symmetry axis and an arbitrary angle θ between the emission dipole and the symmetry axis, can be expressed by a sum of three exponentials. The preexponential factors are given by simple trigonometric functions of the angle θ . The time-resolved fluorescence intensity $I_{||}(t)$, in the case where the $S_1 \rightarrow S_0$ radiative transition decays exponentially, can be written as^{54,55}

$$I_{||}(t) = C[\exp(-t/\tau_n) + 2r_0 \exp(-t/\tau_n) \sum_{i=1}^3 a_i(\theta) \exp(-t/\tau_i^{or})] \quad (5)$$

where C is a proportionality constant, and r_0 is the fluorescence initial anisotropy given in terms of the angle α between the emission and the absorption dipoles by the following equation

$$r_0 = \frac{1}{5}(3 \cos^2 \alpha - 1) \quad (6)$$

The preexponential factors $a_i(\theta)$ are written as

$$a_1(\theta) = \left[\frac{3}{2} \cos^2 \theta - \frac{1}{2} \right]^2 \quad (7a)$$

$$a_2(\theta) = 3 \cos^2 \theta \sin^2 \theta \quad (7b)$$

$$a_3(\theta) = \frac{3}{4} \sin^4 \theta \quad (7c)$$

The reorientational time constants τ_i^{or} are given by

$$\tau_1^{\text{or}} = 1/6D_{\perp} \quad (8a)$$

$$\tau_2^{\text{or}} = 1/(5D_{\perp} + D_{\parallel}) \quad (8b)$$

$$\tau_3^{\text{or}} = 1/(2D_{\perp} + 4D_{\parallel}) \quad (8c)$$

where D_{\parallel} and D_{\perp} are rates of rotation about the symmetry axis and an axis perpendicular to it, respectively. For the emission dipole oriented parallel to the symmetry axis (i.e., $\theta = 0$), a biexponential decay of the temporal fluorescence $I_{\parallel}(t)$ is thus expected

$$I_{\parallel}(t) = C [\exp(-t/\tau_{\text{fl}}) + 2 r_0 \exp(-t/\tau_{\text{fl}} - t/\tau^{\text{or}})] \quad (9)$$

Therefore, the biexponential decay of $I_{\parallel}(t)$ observed for T3, T4, and T5 (see Figure 4), argues that each studied α -oligothiophene in dichloromethane reorients as a prolate ellipsoid and its emission dipole is directed along the long molecular axis. The reorientational time constants, which are summarized in Table 2, are obtained by fitting experimental data to the biexponential function. The fluorescence initial anisotropies of T3, T4, and T5 are also determined to be 0.24 ± 0.04 , 0.28 ± 0.07 , and 0.27 ± 0.06 , respectively.

The stationary fluorescence anisotropies of T3, T4, and T5 in the highly viscous mixture of ethyleneglycol and dimethyl sulfoxide with 1/1 volume ratio have been measured and are of the order of 0.23–0.28, which is comparable to those obtained from the time-resolved fluorescence measurements. This result is expected because in the mixed solvent of ethyleneglycol and dimethyl sulfoxide with 1/1 volume ratio, as we have demonstrated, the molecular reorientation time is much longer than the $S_1 \rightarrow S_0$ radiative decay time (i.e., $\tau_{\text{or}} \gg \tau_{\text{fl}}$). It is also seen that the initial fluorescence anisotropy r_0 does not achieve the theoretical maximum of 0.4 (i.e., $\alpha = 0$). One possible explanation for the reduction of the initial anisotropy is that the absorption dipole is not parallel to the emission dipole. If this is the case, the angle α between the absorption and emission dipoles is estimated to be in the region 26–32°. This result may indicate again the different molecular conformations and electronic structures between the ground and excited states. Further, the values of the initial anisotropy r_0 for T3, T4, and T5 are close to each other, indicating that the orientations of the absorption and emission dipoles are not much affected by varying the oligomer length.

Hydrodynamic Boundary Conditions. A modified Debye–Stokes–Einstein equation is generally used to predict molecular reorientation time, which is dependent on the size and shape of a solute, and the temperature T and the viscosity η of a solvent.⁵⁶ For a prolate ellipsoid for which the emission dipole is oriented along its long axis, the reorientation time can be written as

$$\tau^{\text{or}} = \eta V f / k T g \quad (10)$$

where V is the hydrodynamic volume of the solute molecule, k is the Boltzmann constant, g is the shape factor given by Perrin's equation,⁵⁷ and f is the friction term depending on hydrodynamic boundary conditions. In a stick limit, f is unity; and in a slip limit, f is a function of a molecular axial ratio ranging from zero for a sphere to near unity for a needle-shaped (or disk-shaped) molecule.⁵⁸

To predict the reorientation time based on the modified Debye–Stokes–Einstein equation with either stick or slip condition, we calculate the volume V of each Tn from van der Waals increments,⁵⁹ and estimate the molecular axial ratio ρ (the ratio of a longitudinal axis to an equatorial axis) based on the geometric structure presented by Themans et al.⁵² The parameters used for calculation are summarized in Table 2.

A comparison of reorientation times obtained by experimental measurements to those predicted by the hydrodynamic Debye–Stokes–Einstein model with slip ($\tau_{\text{slip}}^{\text{or}}$) and stick ($\tau_{\text{stick}}^{\text{or}}$) boundary conditions is made in Table 2. Our results demonstrate that the reorientation time predicted by the slip model is in excellent agreement with the experimental measurements for T3, T4, and T5, whereas the stick boundary condition is not successful, indicating weak solvent–solute interactions for these molecules in dichloromethane.

4. Conclusions

In conclusion, the negative second derivative is used to determine the $S_1 \leftarrow S_0$ 0–0 transition energies of Tn for $n = 3, 4, 5$, and 6 in dichloromethane. The $S_1 \leftarrow S_0$ 0–0 transition energy of polythiophene is proposed. The results of the Huang–Rhys analysis of the fluorescence spectra show that the Huang–Rhys parameter decreases with the chain length. This result is associated with the increasing delocalization of the electronic wave functions with increasing the molecular size. The $S_1 \rightarrow S_0$ radiative decay time increases as the chain grows. The observed reorientational relaxation of Tn in dichloromethane at 288 K is consistent with that of an effective prolate ellipsoid of rotation about the axis perpendicular to its symmetry axis, and the rotation about its long molecular axis was not observed, suggesting that the emission transition dipole of Tn is aligned parallel to the long molecular axis. A comparison between the experimental results and the predictions of the Debye–Stokes–Einstein hydrodynamic model with various boundary conditions shows that the hydrodynamic slip model successfully predicts the reorientation times of T3, T4, and T5 in dichloromethane at room temperature.

Acknowledgment. The authors thank Prof. Y. Furukawa, Drs. K. Misawa, M. Yoshizawa, B. Ullrich, and P. Vöhringer, and Prof. C. -Y. King for their helpful discussions. This work was partly supported by a Grant-in-Aid for Specially Promoted Research from the Ministry of Education, Science, Sports, and Culture (No. 05102002) to T.K.

References and Notes

- (1) Kobayashi, T.; Yoshizawa, M.; Stamm, U.; Taiji, M.; Hasegawa, M. *J. Opt. Soc. Am. B* **1990**, 7, 1558.
- (2) Stamm, U.; Taiji, M.; Yoshizawa, M.; Yoshino, K.; Kobayashi, T. *Mol. Cryst. Liq. Cryst.* **1990**, 182A, 147.
- (3) Chen, X.; Ichimura, K.; Fichou, D.; Kobayashi, T. *Chem. Phys. Lett.* **1991**, 185, 286.
- (4) Garnier, F.; Hajlaoui, R.; Yassar, A.; Srivastava, P. *Science* **1994**, 265, 1684.
- (5) Fichou, D.; Nunzi, J. M.; Charra, F.; Pfeffer, N. *Mol. Cryst. Liq. Cryst.* **1994**, 255, 73.
- (6) Periasamy, N.; Danieli, R.; Ruani, G.; Zamboni, R.; Taliani, C. *Phys. Rev. Lett.* **1992**, 68, 919.
- (7) Zamboni, R.; Periasamy, N.; Ruani, G.; Taliani, C. *Synth. Met.* **1993**, 54, 57.
- (8) Noma, N.; Tsuzuki, T.; Shirota, Y. *Adv. Mater.* **1995**, 268, 270.
- (9) Charra, F.; Fichou, D.; Chollet, P. A.; Paquet, D. *Synth. Met.* **1996**, 81, 173.
- (10) Furukawa, Y.; Akimoto, M.; Harada, I. *Synth. Met.* **1987**, 18, 151.
- (11) Yokonuma, N.; Furukawa, Y.; Tasumi, M.; Kuroda, M.; Nakayama, J. *Chem. Phys. Lett.* **1996**, 255, 431.
- (12) Kanemitsu, Y.; Shimizu, N.; Suzuki, K.; Shiraishi, Y.; Kuroda, M. *Phys. Rev. B* **1996**, 54, 2198.

- (13) Watanabe, K.; Asahi, T.; Fukumura, H.; Masuhara, H.; Hamano, K.; Kurata, T. *J. Phys. Chem. B* **1997**, *101*, 1510.
- (14) Birnbaum, D.; Kohler, B. E. *J. Chem. Phys.* **1992**, *96*, 2492.
- (15) Beljonne, D.; Shuai, Z.; Bredas, J. L. *J. Chem. Phys.* **1993**, *98*, 8819.
- (16) Janssen, R. A. J.; Smilowitz, L.; Sariciftci, N. S.; Moses, D. *J. Chem. Phys.* **1994**, *101*, 1787.
- (17) Lopez Navarrete, J. T.; Zerbi, G. *J. Chem. Phys.* **1991**, *94*, 957.
- (18) Negri, F.; Zgierski, M. Z. *J. Chem. Phys.* **1994**, *100*, 2571.
- (19) Lane, P. A.; Wei, X.; Vardeny, Z. V.; Poplawski, J.; Ehrenfreund, E.; Ibrahim, M.; Frank, A. J. *J. Chem. Phys.* **1996**, *210*, 229.
- (20) Verbandt, Y.; Thienpont, H.; Veretennicoff, I.; Rikken, G. L. J. A. *Phys. Rev. B* **1993**, *48*, 8651.
- (21) Thienpont, H.; Rikken, G. L. J. A.; Meijer, E. W.; ten Hoeve, W.; Wynberg, H. *Phys. Rev. Lett.* **1990**, *65*, 2141.
- (22) Hernandez, V.; Casado, J.; Ramirez, F. J.; Zotti, G.; Hotta, S.; Lopez Navarrete, J. T. *J. Chem. Phys.* **1996**, *104*, 9271.
- (23) Evans Christopher, H.; Scaiano, J. C. *J. Am. Chem. Soc.* **1990**, *112*, 2694.
- (24) Fagerstrom, J.; Stafstrom, S. *Phys. Rev. B* **1996**, *54*, 13713.
- (25) Michalitsch, R.; Lang, P.; Yassar, A.; Nauer, G.; Garnier, F. *Adv. Mater.* **1997**, *9*, 321.
- (26) Horowitz, G.; Fichou, D.; Peng, X.; Xu, Z.; Garnier, F. *Solid State Commun.* **1989**, *72*, 381.
- (27) Cornil, J.; Bredas, J. L. *Adv. Mater.* **1995**, *7*, 295.
- (28) Hajlaoui, R.; Horowitz, G.; Garnier, F.; Arce Bouchet, A.; Laigre, L.; El Kassmi, A.; Demanze, F.; Kouki, F. *Adv. Mater.* **1997**, *9*, 389.
- (29) Zerbi, G.; Chierichetti, B.; Ingaras, O. *J. Chem. Phys.* **1991**, *94*, 4646.
- (30) Salaneck, W. R.; Ingnas, O.; Themans, B.; Nilsson, J. O.; Sjogren, B.; Osterholm, J. E.; Bredas, J. L.; Svensson, S. J. *J. Chem. Phys.* **1988**, *89*, 4613.
- (31) Verbandt, Y.; Thienpont, H.; Veretennicoff, I.; Geerlings, P.; Rikken, G. L. J. A. *J. Chem. Phys. Lett.* **1997**, *270*, 471.
- (32) Becker, R. S.; Melo, J. S. D.; Macanita, A. L.; Elisei, F. *Pure Appl. Chem.* **1995**, *67*, 9.
- (33) Bredas, J. L.; Street, G. B.; Themans, B.; Andre, J. M. *J. Chem. Phys.* **1985**, *83*, 1323.
- (34) Chadwick, J. E.; Kohler, B. E. *J. Phys. Chem.* **1994**, *98*, 3631.
- (35) Bredas, J. L.; Heeger, A. J. *Macromolecules* **1990**, *23*, 1150.
- (36) Almenningen, A.; Bastiansen, O.; Svendsas, P. *Acta Chem. Scand.* **1958**, *12*, 1671.
- (37) Samdal, S.; Samuelsen, E. J.; Volden, H. V. *Synth. Met.* **1993**, *59*, 259.
- (38) Bucci, P.; Longeri, M.; Veracini, C. A.; Lunazzi, L. *J. Am. Chem. Soc.* **1974**, *96*, 1305.
- (39) Belletete, M.; Leclerc, M.; Durocher, G. *J. Phys. Chem.* **1994**, *98*, 9450.
- (40) Belletete, M.; Cesare, N. D.; Leclerc, M.; Durocher, G. *J. Chem. Phys. Lett.* **1996**, *250*, 31.
- (41) Chosrovian, H.; Grebner, D.; Rentsch, S.; Naarmann, H. *Synth. Met.* **1992**, *52*, 213.
- (42) Charra, F.; Fichou, D.; Nunzi, J. M.; Pfeffer, N. *J. Chem. Phys. Lett.* **1992**, *192*, 566.
- (43) Grebner, D.; Lap, D. V.; Rentsch, S.; Naarmann, H. *J. Chem. Phys. Lett.* **1994**, *228*, 651.
- (44) Lanzani, G.; Nisoli, M.; De Silvestri, S.; Barbarella, G.; Zambianchi, M.; Tubino, R. *Phys. Rev. B* **1996**, *53*, 4453.
- (45) Kanemitsu, Y.; Suzuki, K.; Masumoto, Y.; Tomiuchi, Y.; Shiraishi, Y.; Kuroda, M. *Phys. Rev. B* **1994**, *50*, 2301.
- (46) Colditz, R.; Grebner, D.; Helbig, M.; Rentsch, S. *J. Chem. Phys.* **1995**, *201*, 309.
- (47) Oelkrug, D.; Egelhaaf, H.-J.; Gierschner, J.; Tompert, A. *Synth. Met.* **1996**, *76*, 249.
- (48) Yang, A.; Hughes, S.; Kuroda, M.; Shiraishi, Y.; Kobayashi, T. *J. Chem. Phys. Lett.* **1997**, *280*, 475.
- (49) Moses, D.; Feldblum, A.; Ehrenfreund, E.; Heeger, A. J. *Phys. Rev. B* **1982**, *26*, 3361.
- (50) Cornil, J.; Beljonne, D.; Shuai, Z.; Hagler, T. W.; Campbell, I.; Bradley, D. D. C.; Bredas, J. L.; Spangler, C. W.; Mullen, K. *J. Chem. Phys. Lett.* **1995**, *247*, 425.
- (51) Sekikawa, T.; Kobayashi, T.; Inabe, T. *J. Phys. Chem. A* **1997**, *101*, 644.
- (52) Themans, B.; Salaneck, W. R.; Bredas, J. L. *Synth. Met.* **1989**, *28*, 359.
- (53) Chung, T.-C.; Kaufman, J. H.; Heeger, A. J.; Wudl, F. *Phys. Rev. B* **1984**, *30*, 702.
- (54) Fleming, G. R.; Morris, J. M.; Robinson, G. W. *J. Chem. Phys.* **1976**, *17*, 91.
- (55) Tao, T. *Biopolymers* **1969**, *8*, 609.
- (56) Jiang, Y.; Blanchard, G. J. *J. Phys. Chem.* **1994**, *98*, 6436.
- (57) Perrin, F. *J. Phys. Radium* **1934**, *5*, 497.
- (58) Hu, C. M.; Zwanzig, R. *J. Chem. Phys.* **1974**, *60*, 4354.
- (59) Edward, J. T. *J. Chem. Educ.* **1970**, *47*, 261.
- (60) Riddick, J. A.; Bunger, W. B. In *Techniques of Chemistry*, Vol. 2: *Organic Solvents*; Weissberger, A., Ed.; John Wiley & Sons: New York, 1970; p 348.